1 **Photoprotection and optimization of sucrose usage contribute to faster recovery**

2 **of photosynthesis after water deficit at high temperatures in wheat**

3

4 **Pedro M. P. Correia[1]*, Anabela Bernardes da Silva[1], Thomas Roitsch[2,3], Elizabete Carmo-Silva[4],**

5 **Jorge Marques da Silva[1]**

6 [1] BioISI – Biosystems & Integrative Sciences Institute, Faculdade de Ciências da Universidade de

7 Lisboa, Campo Grande, 1749-016 Lisboa, Portugal

8 [2] Department of Plant and Environmental Sciences, Section of Crop Science, Copenhagen University,

9 Højbakkegård Allé 13, 2630 Tåstrup, Denmark

10 [3] Department of Adaptive Biotechnologies, Global Change Research Institute, CAS, 603 00 Brno,

11 Czech Republic

12 [4] Lancaster Environment Centre, Lancaster University, Library Avenue, Lancaster, LA1 4YQ, UK

13

14 **Correspondence**

15 *Corresponding author,

16 e-mail: pmpcorreia@fc.ul.pt

17

18 **Abstract**

19 Plants are increasingly exposed to events of elevated temperature and water deficit, which threaten crop

20 productivity. Understanding the ability to rapidly recover from abiotic stress, restoring carbon

21 assimilation and biomass production, is important to unravel crop climate resilience. This study

22 compared the photosynthetic performance of two *Triticum aestivum* L. cultivars, Sokoll and Paragon,

23 adapted to the climate of Mexico and UK, respectively, exposed to one week water deficit and high

24 temperatures, in isolation or combination. Measurements included photosynthetic assimilation rate,

25 stomatal conductance, in vitro activities of Rubisco (EC 4.1.1.39) and invertase (INV, EC 3.2.1.26),

26 antioxidant capacity and chlorophyll *a* fluorescence. In both genotypes, under elevated temperatures

27 and water deficit (WD38°C), the photosynthetic limitations were mainly due to stomatal restrictions

28 and to a decrease in the electron transport rate. Chlorophyll *a* fluorescence parameters clearly indicate

29 differences between the two genotypes in the photoprotection when subjected to WD38°C and showed

30 faster recovery of Paragon after stress relief. The activity of the cytosolic invertase (CytINV) under

31 these stress conditions was strongly related to the fast photosynthesis recovery of Paragon. Taken

32 together, the results suggest that optimal sucrose export/utilization and increased photoprotection of the

33 electron transport machinery are important components to limit yield fluctuations due to water shortage

34 and elevated temperatures.

35

36 *Abbreviations* — A, net photosynthesis assimilation rate; cytINV, cytosolic invertase; ETR, electron
37 transport rate; FRAP, ferric reducing antioxidant power; gs, stomatal conductance; LHCII, Light-
38 harvesting complex II, LRWC, leaf relative water content; LWP, leaf water potential; NPQ, total non-
39 photochemical quenching; PAR, Paragon; Qa, quinone A; Qb, quinone B; qN, non-photochemical
40 quenching; qP, photochemical quenching; RCA, Rubisco activase; RH, relative humidity; RuBP-
41 ribulose 1,5-biphosphate; SOK, Sokoll; SDW, soil dry weight; SFC, soil field capacity; SRWC, soil
42 relative water content; TEAC, Trolox equivalents antioxidant capacity; TSP, Total soluble protein;
43 vacINV, vacuolar invertase; Vi- Rubisco initial activity; Vt- Rubisco total activity; WD, water deficit;
44 WD25℃, water deficit at 25℃; WD38℃, water deficit at 38℃; WW, well-watered; WW25℃, well-
45 watered at 25℃; WW38℃, well-watered at 38℃.

46

47 **Introduction**

48 Global warming is a serious threat to crop production. Wheat is the world's most harvested
49 crop per area, however, wheat yield is below the average of the other major crops (e.g. maize and rice)
50 being therefore only the second most-produced cereal grain, with 26% of the world share (FAOSTAT
51 2017). Around 40% of the global wheat yield fluctuations are explained by climatic variation, and
52 heatwaves and drought are among the principal stressors (Deryng et al. 2014, Zampieri et al. 2017).
53 Each degree-Celsius increase in global mean temperature reduces, on average, the global yield of wheat
54 by 6% (Zhao et al. 2017). To improve wheat yield in a changing climate, and ensure food security for
55 an increasing world population, it is essential to comprehend how wheat plants respond to fluctuations
56 in temperature and water availability, and the mechanisms involved in fast recovery of plant growth
57 upon relief from high temperatures and extended drought.

58 When subjected to high temperatures, plants usually use evaporative cooling to reduce leaf
59 temperature (Carmo-Silva et al. 2012, Costa et al. 2013). However, in response to water shortage, higher
60 plants close the stomata to limit water loss by transpiration. When both conditions are present, stomatal
61 closure reduces transpiration and consequently the plant temperature rises and intercellular CO_2
62 concentration decreases (Chaves et al. 2003, Carmo-Silva et al. 2012, Duque et al. 2013) . High
63 temperatures and drought negatively affect photosynthetic CO_2 fixation at different levels, depending
64 on the stress intensity, decreasing biomass accumulation (Zandalinas et al. 2018, Lamaoui et al. 2018,
65 Tricker et al. 2018, Raja et al. 2020). Even if high temperature increases the maximum rate (Vmax) of
66 the primary carboxylation enzyme of C_3 photosynthesis (Rubisco, EC 4.1.1.39), it also increases the
67 inhibition of Rubisco by sugar phosphate derivatives and thus Rubisco activation state decreases
68 (Salvucci and Crafts-Brandner, 2004a,b). The efficiency of Rubisco depends on the activity of
69 Rubisco's catalytic chaperone, Rubisco Activase (RCA), to promote the release of inhibitory sugar
70 phosphates from active sites. However, RCA is extremely thermal sensitive and depends on the redox
71 status and ADP/ATP ratio (Carmo-Silva et al. 2015). To improve plant tolerance to increased

72 temperatures, bioengineering approaches aiming to enhance Rubisco activity by increasing the
73 thermotolerance of RCA have been suggested (Scafaro et al. 2016, Mueller-Cajar 2017, Shivhare and
74 Mueller-Cajar 2017, Scafaro et al. 2019, Degen et al. 2020). Lower internal CO_2 concentration and high
75 temperatures also reduce Rubisco specificity for CO_2 relative to O_2, resulting in an increase of
76 photorespiration, which leads to the release of previous fixed CO_2 and higher demand for ATP (Walker
77 et al. 2016).

78 Moreover, imbalances between CO_2 assimilation and the rate of light capture usually lead to an
79 excess of energy in the system that can result in reactive oxygen species (ROS) formation and
80 photoinhibition if the capacities of dissipation, scavenging and repairing are exceeded (Yamamoto
81 2016). Among the main energy dissipation mechanisms are the non-photochemical quenching (qN,
82 generally compartmented in three major components, energy-dependent quenching, qE , state-transition
83 quenching, qT, and photoinhibition quenching, qI), cyclic electron flow around photosystem I and
84 chlororespiration (Rumeau et al. 2007, Ruban 2016, Wang and Fu 2016). ROS detoxification is
85 generally conducted enzymatically and by the production of several antioxidant compounds (Mittler et
86 al. 2004; Foyer 2018; Begum et al. 2019) When energy dissipation and ROS detoxification fails,
87 oxidative damage occurs. Many studies reported the reduction of the electron transfer from water to
88 $NADP^+$, due to reversible and irreversible inhibition of photosystem II (PSII) caused by oxidative stress
89 in face of elevated temperatures and/or drought. The main processes involved are the damage of the
90 oxygen-evolving complex (Heckathorn et al. 1998, Tiwari et al. 2008, Chen et al. 2016), the degradation
91 and aggregation of the D1 protein (Kamata et al. 2005, Komayama et al. 2007, Allakhverdiev et al.
92 2008, Takahashi and Murata 2008) and changes on the membrane fluidity (Gounaris et al. 1983,
93 Aronsson et al. 2008, Yamamoto 2016a).

94 Therefore, when photosynthetic performance and plant growth are challenged by water
95 shortage and elevated temperatures, optimization of sucrose export, uptake, and utilization, e.g. through
96 adjustment of source – sink relations via invertase activity (INV, EC 3.2.1.26), can contribute to
97 reducing yield fluctuations. Invertases mediate the hydrolytic cleavage of sucrose into hexose
98 monomers and are involved in regulating carbohydrate partitioning, developmental processes, hormone
99 responses and biotic and abiotic interactions (Roitsch and González 2004). Invertases localized in the
100 vacuole (VacINVs) play a major role in the osmotic regulation (Nägele et al. 2010, Ruan 2014,
101 Weiszmann et al. 2018), while cytosolic invertases (CytINVs) control sugar homeostasis and the
102 maintenance of constant glucose levels to sustain cellular functions (Ruan et al. 2010, Lunn 2016,
103 Figueroa and Lunn 2016).

104 The aims of the present study were to (1) characterise the photosynthetic limitations of two
105 wheat genotypes, Paragon and Sokoll, adapted to distinct climate conditions, under water deficit and/or
106 high temperature, and (2) to determine which factors are responsible for photosynthetic performance
107 and recovery from high temperature in the absence or presence of water deficit. To test the hypothesis
108 that the UK-adapted cultivar Paragon would be less resistant to heat stress and water deficit compared

109 to the Mexican-adapted cultivar Sokoll, the two genotypes were subject to water deficit and elevated
110 temperatures, in isolation or in combination, and compared for net assimilation rate, stomatal
111 conductance, Rubisco and invertase in vitro activities, antioxidant capacity and chlorophyll *a*
112 fluorescence.

113

Materials and methods

Plant growth conditions

116 Two *Triticum aestivum* L. (wheat) genotypes were selected on the basis that these are adapted to distinct
117 climate conditions: Paragon is a traditional UK spring wheat elite cultivar, while Sokoll is a synthetic-
118 derived cultivar developed by the International Maize and Wheat Improvement Centre (CMMYT,
119 Mexico). Plants of both genotypes were grown from seeds in a controlled environment chamber
120 (Fitoclima 5000 EH, Aralab) in 1-L pots containing horticultural substrate (Compo Sana Universal,
121 Compo Sana). Light was provided by fluorescent lamps (Osram Lumilux L 58W/840 cool white lamps)
122 placed at specific distances from the plants to obtain an average photosynthetic photon flux density
123 (PPFD) of 300 μmol m^{-2} s^{-1} at the top of the canopy, with a photoperiod of 16 h. Due to space
124 constraints, temperature assays were performed in two consecutive experiments. After full germination,
125 all plants were initially grown under a control temperature (25/18°C day/night), with 50% relative
126 humidity (RH) for 21 days.

127 For experiments under control temperature, plants remained at 25/18°C (day/night) with 50%
128 RH throughout the experiment. Three weeks post-germination plants were randomly assigned to two
129 irrigation treatments: five plants per cultivar were maintained well-watered (WW; minimum 80% field
130 capacity, WW25°C) throughout the experiment and five plants were subject to water deficit (WD,
131 30±5% field capacity, WD25°C) for 7 days. For experiments under elevated temperature, 21-day-old
132 plants were also exposed to high temperatures (38/31°C day/night) with 60% RH and randomly
133 assigned to the irrigation treatments: ten plants per cultivar were maintained WW (80±5% field
134 capacity, WW38°C) and ten plants were subject to WD (30±5% field capacity, WD38°C) for 5 days.
135 From the 10 plants allocated to WW38°C or WD38°C, 5 were randomly selected for recovery after 5
136 days of stress, re-watered and maintained at control temperatures for 7 days. WD was established by
137 withholding watering and sustaining a minimum of 30±5% field capacity. The soil water content was
138 determined gravimetrically by weighing the pots, and irrigation was provided to compensate
139 evapotranspiration and keep the field capacity in the WW and WD pots. Leaf samples for biochemical
140 analyses were collected at the end of the respective temperature and irrigation treatment, 5-7 h after the
141 beginning of the photoperiod, frozen into liquid nitrogen and stored at -80°C.

142

Leaf and soil water status

144 Plant water status was estimated by leaf relative water content (LRWC) following the methodology
145 described by Čatský (1960). Fresh leaf samples from the flag leaf (1-2 cm^2) were collected, fresh weight

146 was immediately measured in an electronic scale (Sartorius BP221S), turgid weight (LTW) was

147 determined after saturating samples by immersion in deionized water overnight, and dry weight (LDW)

148 was measured after oven-drying samples at 70°C for 48 h. Soil relative water content (SRWC) was

149 determined by following a similar procedure; although soil field capacity (SFC) was achieved by

150 watering the pots to saturation and allowing water drainage for 2 hours, and dry weight (SDW) was

151 measured after oven-drying samples at 110°C for 36 h. Leaf water potential was measured with a C-52

152 thermocouple chamber (Wescor), 20 mm^2 leaf discs were cut and equilibrated for 30 min in the chamber

153 before the readings were recorded by a PSYPRO water potential datalogger (Wescor) in the

154 psychrometric mode.

155

156 **Thermal imaging**

157 Thermal images were obtained using a thermal camera (Flir 50bx, FLIR Systems Inc.) with emissivity

158 set at 0.95 and approximately 1 m distance from the plants. Before each set of measurements,

159 background temperature was determined by measuring the temperature of a crumpled sheet of

160 aluminium foil in a similar position to the leaves of interest with the emissivity set at 1.0 following the

161 methodology described by Costa et al. (2013). Thermal images were analysed with the software FLIR

162 Tools (FLIR Systems, Inc.). The temperature of each plant was determined from the temperature of five

163 leaves using the function "area". Visible images (RGB) were collected to complement the analysis of

164 thermal images.

165

166 **Gas exchange and chlorophyll *a* fluorescence steady-state measurements**

167 Parallel measurements of photosynthetic gas exchange and chlorophyll *a* fluorescence were performed

168 in a non-detached fully expanded leaf from each plant using a gas exchange system (IRGA LCpro+,

169 ADC BioScientific) combined with a chlorophyll fluorescence imaging system (Imaging-PAM

170 Chlorophyll Fluorometer M-series Mini version, Heinz Walz GmbH). Control air temperature was set

171 to 25°C, PPFD at the leaf level set to 226 μmol m^{-2} s^{-1} and the CO_2 concentration in the leaf chamber

172 set to 400 μmol CO_2 mol^{-1} air allowing the leaf to reach steady-state assimilation rate (A) and stomatal

173 conductance (gs). A and gs were calculated by the LCpro+ software according to von Caemmerer and

174 Farquhar (1981). Chlorophyll *a* steady-state fluorescence was analysed using the Imaging Win

175 analytical software (Heinz Walz GmbH). PSII effective quantum yield (ΦPSII) was obtained

176 according to Genty et al. (1989), photochemical (qP) and non-photochemical (qN) quenching were

177 calculated according to Oxborough and Baker (1997) and total non-photochemical fluorescence

178 quenching (NPQ) was calculated using the Stern-Volmer approach (Krause and Jahns 2007). Electron

179 transport rate (ETR) was then calculated as: $ETR = 0.5\Phi$PSII $\times$ PPFD $\times$ abs. Absorptivity (abs) was

180 measured for each leaf before the chlorophyll *a* fluorescence measurement.

181

182 **Chlorophyll *a* fluorescence induction**

183 The kinetics of the rapid fluorescence induction rise was recorded on fully expanded dark-adapted

184 leaves (10 minutes) exposed to a saturating light pulse (3500 µmol m^{-2} s^{-1}) for 1 second to obtain the

185 OJIP Chl a fluorescence transient rise (Handy PEA, Hansatech Instruments). Fluorescence parameters

186 derived from the extracted data, namely specific energy fluxes per QA-reducing PSII reaction center

187 and photosynthetic performance indexes were calculated according to Strasser and collaborators

188 (Strasser et al. 2004, Tsimilli-Michael and Strasser 2008) with the nomenclature presented in Stirbet

189 and Govindjee (2011).

190

191 **Antioxidant capacity**

192 Antioxidant metabolites were extracted from frozen leaf samples (0.1-0.3 g FW) by homogenisation in

193 pure methanol with 1.4 mm zirconium oxide beads (Precellys) in a tissue homogenizer (Precellys

194 Evolution, Precellys) and then centrifuged at 20 000 g for 5 min. Trolox equivalents antioxidant

195 capacity (TEAC) and ferric reducing antioxidant power (FRAP) were measured in the supernatant using

196 a 96-well microtiter plate. TEAC was determined by the reaction of the sample supernatant and 2,2′-

197 Azino-bis (3-ethylbenzothiazoline-6-sulfonic acid) diammonium salt (ABTS), solution 1:20 in

198 phosphate buffer pH 7.4 (0.7-0.8 optical density). The reaction mixtures were incubated 6 min at room

199 temperature before measuring absorbance at 734 nm (ELx808, BioTek Instruments, Inc.). 6-hydroxy-

200 2,5,7,8-tetramethylchroman-2-carboxylic acid (Trolox) standards (0-0.8 mM in 96% ethanol) were

201 measured alongside the samples and used to prepare the respective calibration curve. FRAP was

202 measured by the reaction of the sample supernatant with a solution consisting of 0.3 mM acetate buffer,

203 10 mM 2,4,6-tripyridyl-s-triazine (TPTZ) and 20 mM $FeCl_3$. The reaction mixtures were incubated 4

204 min at room temperature before measuring the absorbance at 593nm (ELx808, BioTek Instruments

205 Inc.). $FeSO_4$ standards (0-1.0 mM) in ddH_2O were measured alongside the samples and used to prepare

206 the respective calibration curves. Samples and standards were measured in triplicate alongside blanks

207 containing no sample.

208

209 **Rubisco activity**

210 Rubisco was extracted from the leaves by grinding frozen samples (0.1-0.3 g FW) in a cold mortar with

211 quartz sand, 1% (w/v) insoluble polyvinylpyrrolidone (PVP), ice-cold extraction medium (1/10 FW per

212 mL) containing 50 mM Bicine-KOH pH 8.0, 1 mM ethylenediaminetetraacetic acid (EDTA), 5% (w/v)

213 polyvinylpyrrolidone (PVP25000), 6% polyethylene glycol (PEG_{4000}), 10 mM 1,4-dithiothreitol (DTT),

214 50 mM β-mercaptoethanol and 1% (v/v) protease inhibitor cocktail for plant extracts (Sigma-Aldrich),

215 adapted from Carmo-Silva et al. (2010). Leaf extracts were then centrifuged at 14 000 g and 4°C for 5

216 min. The supernatant was kept at 4°C and used immediately for measurement of Rubisco activities by

217 the incorporation of $^{14}CO_2$ into acid-stable products at 25 and 38°C, following the protocol described in

218 Parry et al. (1997) with modifications. The reaction mixture contained 100 mM Bicine-NaOH pH 8.2,

219 40 mM $MgCl_2$, 10 mM $NaH^{14}CO_3$ (7.4 kBq $µmol^{-1}$) and 0.4 mM ribulose 1,5-bisphosphate(Ru BP).

220 Rubisco initial activity (Vi) was determined by adding the supernatant to the mixture and stopping the
221 reaction after 60-180s with 10 M HCOOH. Total activity (Vt) was measured after incubating the same
222 volume of extract for 3 min with all the reaction mixture components except RuBP, to allow
223 carbamylation of all the Rubisco available catalytic sites. The reaction was then started by adding RuBP
224 and stopped as above. All measurements were carried out in triplicate and control reactions were
225 quenched with HCOOH prior to the addition of RuBP. The mixtures were completely dried at 70°C
226 overnight and the residues re-hydrated in 0.5 mL ddH$_2$O, then mixed with 5 mL scintillation cocktail
227 (Ultima Gold, Perkin-Elmer). Radioactivity due to ^{14}C incorporation in the acid-stable products was
228 measured by liquid scintillation counting (LS7800, Beckman). The activation state of Rubisco was
229 calculated as the ratio Vi / Vt × 100. Total soluble protein (TSP) content was determined according to
230 the Bradford method (Bradford 1976) using BSA Fraction V as standard protein.
231

Invertase activity

233 Cytosolic invertase (CytInv) and vacuolar invertase (VacInv) were extracted from the leaves by
234 grinding frozen samples (0.1-0.3 g FW) in a cold mortar with quartz sand, 1% (w/v) PVPP, ice-cold
235 extraction medium containing 40 mM TRIS-HCl pH 7.6, 3 mM MgCl$_2$, 1 mM EDTA, 0.1 mM
236 phenylmethylsulfonyl fluoride (PMSF), 1 mM benzamidine, 14 mM β-mercaptoethanol, 24 μM
237 nicotinamide adenine dinucleotide phosphate (NADP$^+$), according to Jammer et al. (2015), with
238 modifications. Leaf extracts were then centrifuged at 20 000 g for 10 min at 4°C. The supernatant was
239 kept at 4°C and dialysed overnight with 20 mM potassium phosphate buffer pH 7.4 at 4°C in a dark
240 room. Extracts were aliquoted, frozen in liquid nitrogen and stored at -20°C. The activities were
241 measured in thawed samples using 96-well microtiter plates. Reaction mixtures containing 10 mM
242 sucrose and dialysed protein extract were incubated for 30 min at 37°C, cooled for 5 min on ice to stop
243 the reaction, and then incubated for 30 min at room temperature with GOD-POD reagent (10 U mL^{-1}
244 of Glucose oxidase from *Aspergillus niger* (GOD), 0.8 U mL^{-1} peroxidase from horseradish (POD) and
245 0.8 mg mL^{-1} ABTS in 0.1 M potassium phosphate buffer (pH 7.0). The amount of liberated glucose
246 was determined by measurement of absorbance at 405 nm at 30°C (ELx808, BioTek Instruments Inc.).
247 Glucose standards (0-50 nmol) were measured alongside the samples and used to prepare the respective
248 calibration curves. All measurements were carried out in triplicate alongside blanks containing no
249 sucrose. TSP content was determined according to the Bradford method (Bradford 1976) using BSA
250 Fraction V as standard protein.
251

Statistical analysis

253 The statistical significance of trait variation was tested by factorial ANOVA, with cultivars, irrigation
254 and temperature regimes as fixed factors. Post-hoc comparison between treatments was performed with
255 Duncan test ($P < 0.05$) using IBM SPSS Statistics, Version 25 (IBM, USA). Multivariate analysis was
256 performed with MixOmics R package (Rohart et al. 2017) using Rstudio software.

257

Results

Leaf and soil water relations under drought and high temperatures

To characterise the leaf and soil water status of Sokoll and Paragon plants, leaf and soil relative water content (LRWC and SRWC, respectively) and leaf water potential (LWP) were estimated at the end of each experimental condition (Table 1). Well-watered (WW) plants presented leaf relative water content (LRWC) and leaf water potential (LWP) around or above 80% and -1 M Pa, respectively, suggesting good cellular hydration. On the other hand, water deficit (WD) conditions led to a decrease in LRWC and LWP values (lower than 70% and -1 MPa, respectively), revealing a reduction in hydration and a considerable driving force for water movement through the plant. Under WD25°C, Paragon presented higher LRWC than Sokoll, even though no significant differences were found for LWP and soil relative water content (SRWC), showing the capacity of this genotype to maintain cellular hydration under these conditions. The canopy temperature (Tcanopy) increased in both cultivars when subject to high temperatures. Under WW38°C, Tcanopy was significantly lower in Sokoll compared to Paragon, indicating the ability of Sokoll to avoid heat and maintain optimal cell temperature. No differences were observed between the genotypes when subjected to WD38°C, the observed LRWC under 50% and low LWP indicate severe drought stress, and Tcanopy was also highest in these plants.

Effects of drought and high temperature on photosynthesis

WD plants had significantly lower net photosynthesis assimilation rate (A), stomatal conductance (gs) and electron transport rate (ETR) compared to WW plants, except for Paragon at 25°C (Fig. 1A-C). Steady-state photosynthetic gas-exchanges were comparable for both genotypes under WW conditions. A strong positive relationship between A and gs was observed (r=0.914, P<0.0001 and r=0.974 P<0.0001, Paragon and Sokoll respectively, Table S1), suggesting a possible stomatal limitation to photosynthesis, and between A and ETR (r= 0.966, P<0.0001 and r=0.797, P<0.0001, Table S1), suggesting limitations at the photosystems level.

Effect of water deficit and high temperatures on Rubisco in vivo activities measured at control and high temperatures

To verify if the limitations in the carbon fixation found under stress conditions were a result of an imbalance in the Calvin-Benson-Bassham cycle, the in vivo Rubisco activity was assessed at the two growth temperatures. When Rubisco activity was measured at 25°C, the initial and total velocities decreased significantly under WD (WD25°C and WD38°C) and elevated temperatures (WW38°C) (Fig. 2A,B). However, the activation state of Rubisco remained largely unchanged between the various conditions (Fig. 2C). When Rubisco assays were performed at 38°C, activities were higher compared to measurements at 25°C, although the increase of initial velocity was higher than in total velocity (Fig. 2D,E). A significant difference was also observed between plants grown at 38°C under different

294 irrigation regimes. No significant differences were observed in Rubisco activation state when measured

295 at this temperature (Fig. 2F). The lack of differences in net photosynthetic assimilation rate of WW38°C

296 plants (Fig. 1A) would indicate that even the reduced level of Rubisco activity in these plants (~10 µmol

297 CO_2 m^{-2} s^{-1}, Fig. S1D) is sufficient to support photosynthesis at the growth light levels (PPFD <300

298 µmol photons m^{-2} s^{-1}).

299

300 **Effect of water deficit and high temperatures on the antioxidant capacity and chlorophyll *a***

301 **fluorescence**

302 To analyse how both genotypes cope with possibly harmful consequences caused by energy excess

303 under stress, chlorophyll *a* fluorescence and two dissipation mechanisms, ROS scavenging and non-

304 photochemical dissipation, were quantified. A decrease of photochemical quenching (qP) was observed

305 in Sokoll WD25°C and in both genotypes at WD38°C (Fig. 3A-B). Under the same conditions, non-

306 photochemical quenching (qN, NPQ) increased (Fig. 3 C-D). Moreover, the two genotypes showed an

307 increase in the antioxidant capacity (FRAP and TEAC) under drought at both temperatures (Fig. 3 E,

308 F). In order to thoroughly understand how the different biochemical processes in the photosystems are

309 affected by stress conditions, the chlorophyll *a* kinetic parameters were correlated with the antioxidant

310 capacity and NPQ, and ETR (Fig. 4). A positive correlation was observed between the antioxidant

311 capacity and NPQ, as well as an inverse correlation to ETR. In all conditions, Sokoll showed a stronger

312 correlation between the number of electron carriers per electron transport chain (S_m) and ETR than

313 Paragon. The strength of the correlation between energy fluxes (J^{ABS}, J^{DI}, J_o^{ET2} and J_o^{RE1}), ETR and NPQ

314 changed for both genotypes under WD (Fig. 4A,C). This was particularly the case in Paragon in

315 WD38°C (Figs 4C,S2 and Table S2), supported by the increase of J^{ABS}, J^{DI} and J_o^{RE1} to control

316 conditions. In Sokoll the positive correlation between ETR and both electron transport fluxes (J_o^{ET2} and

317 J_o^{RE1}, Fig. 4C) indicated a decrease of electron transport rate on the entire flux until photosystem I.

318

319 **Recovery from high temperatures conditions**

320 Following 5 days of exposure to high temperatures and/or drought, wheat plants were allowed to recover

321 for 7 days (at 25°C and WW) and their photosynthetic performance was compared by measuring

322 chlorophyll *a* fluorescence, net photosynthetic assimilation and stomatal conductance. Even though no

323 differences were detected on the fraction of open PSII reaction centres (qP, Fig. 5A,B), a significant

324 increase on the non-photochemical quenching was observed relative to control (qN, NPQ, Fig. 5A,C,D).

325 The increase in NPQ was only accompanied by a decrease in the electron transport rate of Sokoll

326 recovering from WD38°C (Fig. 5E). Paragon presented higher LRWC and LWP when recovering from

327 WD38°C than Sokoll (Table 1), even though no significant differences were found, indicating a higher

328 capacity of this genotype to return to control cellular hydration and recover the driving force for water

329 movement through the plant. Slower recovery of Sokoll ETR and higher NPQ suggest that WD is

330 promoting photoinhibition in Sokoll. The photosynthetic assimilation rate and stomatal conductance

331   (Fig. 5F,G) increased in Paragon plants recovered after growing at 38°C in WW and WD conditions

332   relative to control. However, in Sokoll, the photosynthetic assimilation rate decreased significantly in

333   recovery from WD38°C and gs decreased when recovering from both conditions. All parameters

334   reflecting the photosynthetic capacity revealed a better recovery from WD38°C in Paragon compared

335   to Sokoll. Once again, results suggest that stomatal conductance impairment and recovery are a limiting

336   factor for photosynthesis rate under water deficit and high temperature.

337

338   **Invertase in vivo activities under water deficit and high temperatures**

339   To verify if other sources of energy were used to cope with stress besides the direct usage of

340   photoassimilates, the activity of invertases isoenzymes (located in the cytosol and vacuole) were

341   measured. Results showed that the activity of vacINV was higher in Paragon for all the conditions

342   compared to Sokoll (Fig. 6A). However, modulation of cytINV was observed according to different

343   stress conditions (Fig. 6B): the cytINV activity increased in plants growing at 38°C with an interesting

344   difference between WD38°C to WW38°C and WW25°C in Paragon. Even though the CytINV activity

345   slightly increased, no significant differences were found for all conditions in Sokoll (Fig 6B). Overall,

346   in Paragon, cytINV was negatively correlated to the assimilation rate (r=-0.774, P<0.0001, Table S1).

347   Together with the previous results that showed a better recovery of this genotype after the combination

348   of water deficit and high temperature, these data suggest that an increase of sucrose catabolism, when

349   the production of photosynthetic assimilates decreases, improved wheat recovery from stress

350   conditions.

351

352   **Discussion**

353   Two wheat cultivars, Paragon and Sokoll, were studied for their ability to withstand water

354   deficit and high temperatures, in isolation or in combination. Paragon is a traditional UK spring wheat

355   elite cultivar (Moore 2015), while Sokoll is a synthetic-derived cultivar developed by the International

356   Maize and Wheat Improvement Centre (CIMMYT, Mexico), known to show good productivity under

357   elevated temperatures (Solís Moya and Camacho Casas 2016). As these genotypes are adapted to

358   distinct environmental conditions, it is of relevance to determine which factors are responsible for their

359   photosynthetic performance. Therefore, the present study aimed to first characterise the photosynthetic

360   limitations of the two genotypes under water deficit and/or high temperature and then to assess

361   photosynthetic recovery from high temperature in the absence or presence of drought. To achieve this

362   goal, Paragon and Sokoll were compared using several established parameters, namely net assimilation

363   rate, stomatal conductance, Rubisco and invertase in vitro activities, antioxidant capacity and

364   chlorophyll *a* fluorescence.

365   Under increased temperatures a natural heat avoidance strategy of plants is to decrease leaf

366   temperature through increased transpiration (Carmo-Silva et al. 2012, Zandalinas et al. 2018). Albeit at

367 25°C, both genotypes showed a mean leaf temperature slightly higher than the atmospheric temperature

368 (Paragon = 26.87°C; Sokoll = 26.33°C), when subjected to 38°C both genotypes showed a decrease of

369 leaf temperature relative to atmospheric temperature, which was statistically significant in Sokoll at

370 WW38°C (Table 1). Additionally, both genotypes maintained similar photosynthetic assimilation and

371 electron transport rates compared to control conditions (Fig. 1A,C). However, in vitro Rubisco activity

372 decreased more than 10-fold (Fig. 2), in agreement with previous reports (Galmés et al. 2013, Perdomo

373 et al. 2016, 2017). The maintenance of assimilation rates despite this abrupt decline in Rubisco activity

374 can be explained by the increase in catalytic rate under increased temperature. When measured at 38°C,

375 the initial activity was 5 times higher than when measured at 25°C (Fig. 2A,D) and showed rates

376 comparable to the rates of photosynthesis in the same plants. In vivo, the Rubisco chaperone (RUBISCO

377 ACTIVASE, RCA) helps to overcome possible dead-end inhibition of Rubisco by promoting ATP-

378 dependent conformational changes at the closed sites of Rubisco (Feller, Crafts-Brandner and Salvucci,

379 1998, Crafts-Brandner and Salvucci, 2000, Salvucci and Crafts-Brandner, 2004) and may contribute to

380 sustaining Rubisco activities at adequate levels to support carbon assimilation (Perdomo et al. 2017).

381 Under our experimental conditions and without water restrictions, photosynthesis occurred at sufficient

382 rates to supply carbon for cellular growth and metabolic energy.

383 Despite no direct impact of high temperatures was found on photosynthetic assimilation,

384 stomatal conductance and electron transport rate, and in spite of the better performance of Paragon at

385 WD25°C, no differences between genotypes were observed at WD38°C, since these parameters

386 significantly decreased in both Paragon and Sokoll (Fig. 1A,C). These results illustrate that when

387 combined, water deficit and high temperatures have a synergistic effect, both genotypes showed severe

388 leaf dehydration (LRWC> 50%, Table 1) and a serious reduction of stomatal conductance (less than

389 15% of control values, Fig. 1B). Under such stress conditions, photosynthesis no longer provides a

390 source of carbon and other mechanisms are required to enable plants' intense reprogramming effort to

391 acclimatise, survive and, mostly, to recover physiological functions after re-watering. Various stress

392 conditions result in the coordinated regulation of both source - sink relations and direct defence

393 responses (Roitsch 1999, Jan et al. 2019, Kosar et al. 2020). Notably, the activities of the different

394 invertase isoenzymes are affected by drought and heat stress (Albacete et al. 2011). Paragon recovered

395 faster from high temperatures and water deficit conditions (Fig. 5) presented higher activity of cytINV

396 and slightly higher activity of vacINV (Fig. 6A,B). These results are suggesting that genotypes with

397 high capacity to hydrolyse sucrose recover faster from episodes of high temperatures combined with

398 drought and therefore reduce the impact of climate fluctuation in yield. Marques da Silva and Arrabaça

399 (2004), in the C_4 grass *Setaria sphacelata*, found that the higher amount of soluble carbohydrates and t

400 lower amount of starch in leaves exposed to long-term water deficit played a minor role on the

401 osmoregulation against desiccation, suggesting that high availability of hexoses is mainly due to

402 changes on the sucrose metabolism to support other cellular functions. Pinheiro and Chaves (2011) also

403 suggested a connection between cytINV and ABA, sucrose, starch, and ROS metabolism in response

404   to acute drought stress. Higher activity of vacINV has been reported in maize leaves under water
405   deprivation conditions (Pelleschi et al. 1997, Trouverie et al. 2003), although in sugarcane (Wang et al.
406   2017), cytINV was also shown to play a more prominent role than vacINV under abiotic stress. In
407   barley, activities of both vacINV and cytINV were repressed after a heat stress episode (Antonio Cuesta-
408   Seijo et al. 2019). In tomato, ectopic expression of cell wall invertases resulted in drought tolerance that
409   was accompanied by also changes in cytINV and vacINV (Albacete et al. 2015). Barratt et al. (2009)
410   demonstrated that cytINV may be the primary route by which carbon from sucrose is supplied to non-
411   photosynthetic tissues in Arabidopsis, suggesting, in concordance to our results, that it would grant a
412   source of carbon to feed cellular functions when photosynthesis is impaired. Secchi and Zwieniecki
413   (2012, 2016) suggested that, under severe drought, high levels of sugar accumulation and invertase
414   activity could prime the xylem for the accelerated restoration of xylem function upon return to hydrated
415   conditions. The authors proposed that the reduction of stomatal conductance and embolism reduces the
416   transpiration flow, subsequently changing the balance of carbohydrate fluxes in xylem instigating the
417   accumulation of sucrose in the apoplast. That mechanism can trigger a cellular stress response
418   promoting starch degradation, leading to the increase of cellular soluble sugar concentration and
419   membrane sucrose gradient. The suggested model is in accordance to our results, Paragon showed high
420   activity of invertases under severe drought (WD38°C, Fig. 6) and the resuming high osmotic level could
421   help xylem embolism refilling and the recovery of transport. When water is delivered from roots, the
422   fast recovery of transpiration could consequently help to explain the faster recovery of photosynthesis,
423   leaf water potential and leaf hydration (Fig. 5 and Table 1). The observed evidence highlighted the role
424   of sucrolytic enzymes in the supply of carbon from sucrose needed to the massive metabolic
425   reorganization employed to tolerate stress, helping plants to recover faster and being less affected by
426   heat and water deficit episodes.

427   In the present study, WD38°C affected the photochemical capacity in both genotypes,
428   increasing NPQ and qN (Fig. 3B,C) and decreasing qP (Fig. 3A), followed by a decrease of ETR (Fig.
429   1C). Generally, in higher plants, qE is assumed as the major component of qN, as a short time adaptation
430   to deal with the overproduction of ATP and NADPH and the accumulation of protons in the thylakoid
431   lumen when CO_2 fixation decreases (Krause and Jahns 2007, Takahashi and Murata 2008). Generally,
432   if the energy dissipation mechanisms (qE, qT) and ROS detoxification fail, oxidative damage occurs,
433   leading to photoinhibition (Murata et al. 2007, Yamamoto 2016). The increase in the ROS scavenging
434   activity was observed in both genotypes under WD38°C (Fig. 3E,F). In Paragon, an increase of the
435   absorbed photon flux (J^{ABS}) was not followed by an increase in the maximum trapped flux (J_o^{TR}) and
436   the electron transport from Q_A to Q_B (J_o^{ET2}), probably because of the observed increase in the dissipated
437   energy flux (J^{DI}) (Figs 4, S2 and Table S2), which avoid the overreduction of the electron transport
438   chain. Additionally, the photochemical function of this genotype fully recovered upon stress release, as
439   shown by the recovery of qP and ETR to values similar to control conditions (Fig. 5B,E). The increase
440   in dissipated energy flux may be related to a photoprotective mechanism based on the aggregation and

detachment of the light-harvesting complex II (LHCII) from the reaction center of PSII (Ruban et al. 2012; Ruban 2016). In higher plants, LHCII aggregates are common sites of energy dissipation facilitated by PsbS (qE) or induced by redox-controlled LHCII phosphorylation (qT) (Minagawa 2011), active in plants under CO_2 starvation and heat stress (Šiffel and Vácha 1998, Šiffel and Braunová 1999, Tang et al. 2007). On the other hand, in Sokoll, the reduction of ETR highly correlates to the decrease of both electron transport fluxes (JoET2 and JoRE1, Fig. 4 WD38°C), and despite the full recovery of qP, NPQ levels remained at high levels and ETR stayed below control condition, indicating slower and limited recovery (Fig. 5). Chlorophyll fluorescence parameters clearly indicate differences in photoprotection when both genotypes were subjected to WD38°C and faster recovery of Paragon after stress relief.

Modulation of the cytosolic invertase was observed and suggests a relationship between an increase of CytINV activity under stress and the recovery of photosynthesis upon high temperatures and water deficit conditions. Upon water shortage and elevated temperatures, when photosynthetic performance and growth priorities are altered, optimization of sucrose export and utilization in conjunction with increased photoprotection of the electron transport machinery could contribute to the recovery of photosynthetic capacity, and consequently to reduce yield fluctuations under climate change. The integration of cell physiological phenotyping via the semi-highthroughput determination of enzyme activity signatures (Jammer et al. 2015) with ecophysiological measurements proved to be a powerful holistic phenomics approach (Großkinsky et al. 2015).

Author contributions

P.M.P.C. planned and carried out the experiments, analysed and interpreted the results. E.C.S. and J.M.S. contributed to the interpretation of the results and supervised the research. A.B.S. and T.R. provided critical feedback. P.M.P.C. took the lead in writing the manuscript. All authors discussed the results and contributed to the final manuscript.

478

Data availability statement

The data that support the findings of this study are available from the corresponding author upon request and data supporting findings of this study are available in the supplementary material of this article.

482

References

Albacete A, Cantero-Navarro E, Großkinsky DK, Roitsch T (2015) Ectopic overexpression of the cell wall invertase gene CIN1 leads to dehydration avoidance in tomato. J Exp Bot 66: 863–878

Albacete A, Großkinsky DK, Roitsch T (2011) Trick and treat: a review on the function and regulation of plant invertases in the abiotic stress response. Phyton Annales Rei Botanicae 50: 181-204

Allakhverdiev SI, Kreslavski VD, Klimov VV, Los DA, Carpentier R, Mohanty P (2008) Heat stress: An overview of molecular responses in photosynthesis. Photosynth Res 98: 541–550

Cuesta-Seijo AJ, De Porcellinis AJ, Valente AH, Striebeck A, Voss C, Marri L, Hansson A, Jansson AM, Dinesen MH, Fangel JU, Harholt J, Popovic M, Thieme M, Hochmuth A, Zeeman SC, Mikkelsen TN, Jørgensen RB, Roitsch T, Lindberg MB, Braumann I (2019) Amylopectin Chain Length Dynamics and Activity Signatures of Key Carbon Metabolic Enzymes Highlight Early Maturation as Culprit for Yield Reduction of Barley Endosperm Starch after Heat Stress. Plant Cell Physiol 60: 2692–2706

Aronsson H, Schöttler MA, Kelly AA, Sundqvist C, Dörmann P, Karim S, Jarvis P (2008) Monogalactosyldiacylglycerol deficiency in Arabidopsis affects pigment composition in the prolamellar body and impairs thylakoid membrane energization and photoprotection in leaves. Plant Physiol 148: 580–592

Barratt DHP, Derbyshire P, Findlay K, Pike M, Wellner N, Lunn J, Feil R, Simpson C, Maule AJ, Smith AM, (2009) Normal growth of Arabidopsis requires cytosolic invertase but not sucrose synthase. Proc Natl Acad Sci USA 106: 13124–13129

Begum N, Ahanger MA, Su Y, Lei Y, Mustafa NSA, Ahmad P, Zhang L (2019) Improved drought tolerance by AMF inoculation in maize (*Zea mays*) involves physiological and biochemical implications. Plants 8: 579

Bradford MM (1976) A rapid and sensitive method for the quantitation of microgram quantities of protein utilizing the principle of protein-dye binding. Anal Biochem 72: 248–254

Carmo-Silva AE, Gore MA, Andrade-Sanchez P, French NA, Hunsaker DJ, Salvucci ME (2012) Decreased CO2 availability and inactivation of Rubisco limit photosynthesis in cotton plants under heat and drought stress in the field. Environ Exp Bot 83: 1–11

Carmo-Silva AE, Keys AJ, Andralojc PJ, Powers SJ, Arrabaça MC, Parry MAJ (2010) Rubisco activities, properties, and regulation in three different C4 grasses under drought. J Exp Bot 61: 2355–2366

Carmo-Silva E, Scales JC, Madgwick PJ, Parry MAJ (2015) Optimizing Rubisco and its regulation for

514   greater resource use efficiency. Plant, Cell Environ 38: 1817–1832

515   Čatský J (1960) Determination of water deficit in disks cut out from leaf blades. Biol Plant 2:76–78

516   Chaves MM, Maroco JP, Pereira JS (2003) Understanding plant responses to drought - from genes to
517   the whole plant. Funct Plant Biol 30: 239

518   Chen YE, Liu WJ, Su YQ, Cui JM, Zhang ZW, Yuan M, Zhang HY, Yuan S (2016) Different response
519   of photosystem II to short and long-term drought stress in *Arabidopsis thaliana*. Physiol Plant
520   158: 225–235

521   Costa JM, Grant OM, Chaves MM (2013) Thermography to explore plant-environment interactions. J
522   Exp Bot 64: 3937–3949

523   Crafts-Brandner SJ, Salvucci ME (2000) Rubisco activase constrains the photosynthetic potential of
524   leaves at high temperature and CO_2. Proc Natl Acad Sci USA 97: 13430–13435

525   Degen GE, Worrall D, Carmo-Silva E (2020) An isoleucine residue acts as a thermal and regulatory
526   switch in wheat Rubisco activase. Plant J 103: 742–751

527   Deryng D, Conway D, Ramankutty N, Price J, Warren R (2014) Global crop yield response to extreme
528   heat stress under multiple climate change futures. Environ Res Lett 9: 034011

529   Duque AS, de Almeida AM, Bernardes da Silva A, Marques da Silva J, Farinha PA, Santos D, Fevereiro
530   P, Araújo SS (2013) Abiotic Stress Responses in Plants: Unraveling the Complexity of Genes and
531   Networks to Survive. InTech 3: 49-101

532   FAOSTAT Statistical Database; 2017; Food and Agriculture Organization of the United Nations; Rome

533   Feller U, Crafts-Brandner SJ, Salvucci ME (1998) Moderately High Temperatures Inhibit Ribulose-
534   1,5-Bisphosphate Carboxylase/Oxygenase (Rubisco) Activase-Mediated Activation of Rubisco.
535   Plant Physiol 116: 539–46

536   Figueroa CM, Lunn JE (2016) A tale of two sugars: Trehalose 6-phosphate and sucrose. Plant Physiol
537   172: 7–27

538   Foyer CH (2018) Reactive oxygen species, oxidative signaling and the regulation of photosynthesis.
539   Environ Exp Bot 154: 134–142

540   Galmés J, Aranjuelo I, Medrano H, Flexas J (2013) Variation in Rubisco content and activity under
541   variable climatic factors. Photosynth. Res 117: 73–90

542   Genty B, Briantais JM, Baker NR (1989) The relationship between the quantum yield of photosynthetic
543   electron transport and quenching of chlorophyll fluorescence. Biochim Biophys Acta 990:87–92

544   Gounaris K, Brain APR, Quinn PJ, Williams WP (1983) Structural and functional changes associated
545   with heat-induced phase-separations of non-bilayer lipids in chloroplast thylakoid membranes.
546   FEBS Letters 153: 47-52

547   Großkinsky DK, Svensgaard J, Christensen S, Roitsch T (2015) Plant phenomics and the need for
548   physiological phenotyping across scales to narrow the genotype-to-phenotype knowledge gap. J
549   Exp Bot 66: 5429-40

550   Heckathorn SA, Coleman JS, Hallberg RL (1998) Recovery of net CO_2 assimilation after heat stress is

correlated with recovery of oxygen-evolving-complex proteins in *Zea mays* L. Photosynthetica 34: 13–20

Jammer A, Gasperl A, Luschin-Ebengreuth N, Heyneke E, Chu H, Cantero-Navarro E, Großkinsky DK, Albacete AA, Stabentheiner E, Franzaring J, Fangmeier A, Graaff E, Roitsch T (2015) Simple and robust determination of the activity signature of key carbohydrate metabolism enzymes for physiological phenotyping in model and crop plants. J Exp Bot 66: 5531–5542

Jan S, Abbas N, Ashraf M, Ahmad P (2019) Roles of potential plant hormones and transcription factors in controlling leaf senescence and drought tolerance. Protoplasma 256: 313–329

Kamata T, Hiramoto H, Morita N, Shen JR, Mann NH, Yamamoto Y (2005) Quality control of photosystem II: An FtsH protease plays an essential role in the turnover of the reaction center D1 protein in Synechocystis PCC 6803 under heat stress as well as light stress conditions. Photochem Photobiol Sci 4: 983–990

Komayama K, Khatoon M, Takenaka D, Horie J, Yamashita A, Yoshioka M, Nakayama Y, Yoshida M, Ohira S, Morita N, Velitchkova M, Enami I, Yamamoto Y (2007) Quality control of Photosystem II: Cleavage and aggregation of heat-damaged D1 protein in spinach thylakoids. Biochim Biophys Acta - Bioenerg 1767: 838–84

Kosar F, Akram NA, Ashraf M, Ahmad A, Alyemeni MN, Ahmad P (2020) Impact of exogenously applied trehalose on leaf biochemistry, achene yield and oil composition of sunflower under drought stress. Physiol Plant https://doi.org/10.1111/ppl.13155

Krause GH, Jahns P (2007) Non-photochemical Energy Dissipation Determined by Chlorophyll Fluorescence Quenching: Characterization and Function. In: Papageorgiou G.C., Govindjee (eds) Chlorophyll a Fluorescence. Advances in Photosynthesis and Respiration, vol 19. Springer, Dordrecht 463–495

Lamaoui M, Jemo M, Datla R, Bekkaoui F (2018) Heat and drought stresses in crops and approaches for their mitigation. Front Chem 6: 26

Lunn JE (2016) Sucrose Metabolism. In: eLS. John Wiley & Sons, Ltd, Chichester, UK, pp 1–9

Marques da Silva J, Arrabaça MC (2004) Contributions of soluble carbohydrates to the osmotic adjustment in the C4 grass *Setaria sphacelata*: A comparison between rapidly and slowly imposed water stress. J Plant Physiol 161: 551–555

Minagawa J (2011) State transitions-the molecular remodeling of photosynthetic supercomplexes that controls energy flow in the chloroplast. Biochim Biophys Acta - Bioenerg. 1807: 897–905

Mittler R, Vanderauwera S, Gollery M, Van Breusegem F (2004) Reactive oxygen gene network of plants. Trends Plant Sci 9: 490–498

Moore G (2015) Strategic pre-breeding for wheat improvement. Nat Plants 1: 15018

Mueller-Cajar O (2017) The diverse AAA+ machines that repair inhibited Rubisco active sites. Front Mol Biosci 4

Murata N, Takahashi S, Nishiyama Y, Allakhverdiev SI (2007) Photoinhibition of photosystem II under

environmental stress. Biochim Biophys Acta - Bioenerg. 1767: 414–421

Nägele T, Henkel S, Hörmiller I, et al (2010) Mathematical modeling of the central carbohydrate metabolism in arabidopsis reveals a substantial regulatory influence of vacuolar invertase on whole plant carbon metabolism. Plant Physiol 153: 260–272

Oxborough K, Baker NR (1997) Resolving chlorophyll a fluorescence images of photosynthetic efficiency into photochemical and non-photochemical components - Calculation of qP and Fv'/Fm' without measuring Fo'. Photosynth Res 54: 135–142

Parry MAJ, Andralojc PJ, Parmar S, Keys AJ, Habash D, Paul, MJ, Alred R, Quick WP, Servaites JC (1997) Regulation of Rubisco by inhibitors in the light. Plant, Cell Environ 20: 528–534

Pelleschi S, Rocher JP, Prioul JL (1997) Effect of water restriction on carbohydrate metabolism and photosynthesis in mature maize leaves. Plant, Cell Environ 20: 493–503

Perdomo JA, Capó-Bauçà S, Carmo-Silva E, Galmés J (2017) Rubisco and Rubisco Activase Play an Important Role in the Biochemical Limitations of Photosynthesis in Rice, Wheat, and Maize under High Temperature and Water Deficit. Front Plant Sci 8: 490

Perdomo JA, Carmo-Silva E, Hermida-Carrera C, Flexas J, Galmés J (2016) Acclimation of Biochemical and Diffusive Components of Photosynthesis in Rice, Wheat, and Maize to Heat and Water Deficit: Implications for Modeling Photosynthesis. Front Plant Sci 7: 1–16

Pinheiro C, Chaves MM (2011) Photosynthesis and drought: Can we make metabolic connections from available data? J Exp Bot 62: 869–882

Raja V, Qadir SU, Alyemeni MN, Ahmad P (2020) Impact of drought and heat stress individually and in combination on physio-biochemical parameters, antioxidant responses, and gene expression in *Solanum lycopersicum*. 3 Biotech 10:208

Rohart F, Gautier B, Singh A, Lê Cao K-A (2017) mixOmics: An R package for 'omics feature selection and multiple data integration. PLOS Comput Biol 13: e1005752

Roitsch T (1999) Source-sink regulation by sugar and stress. Curr Opin Plant Biol 2: 198–206

Roitsch T, González MC (2004) Function and regulation of plant invertases: Sweet sensations. Trends Plant Sci 9: 606–613

Ruan Y-L (2014) Sucrose Metabolism: Gateway to Diverse Carbon Use and Sugar Signaling. Annu Rev Plant Biol 65: 33-67

Ruan YL, Jin Y, Yang YJ, Li GJ, Boyer JS (2010) Sugar input, metabolism, and signaling mediated by invertase: Roles in development, yield potential, and response to drought and heat. Mol Plant 3: 942–955

Ruban AV (2016) Nonphotochemical chlorophyll fluorescence quenching: Mechanism and effectiveness in protecting plants from photodamage. Plant Physiol 170: 1903-16

Ruban A V., Johnson MP, Duffy CDP (2012) The photoprotective molecular switch in the photosystem II antenna. Biochim Biophys Acta - Bioenerg 1817: 167–181

Rumeau D, Peltier G, Cournac L (2007) Chlororespiration and cyclic electron flow around PSI during

photosynthesis and plant stress response. Plant, Cell Environ 30: 1041–1051

Salvucci ME, Crafts-Brandner SJ (2004a) Inhibition of photosynthesis by heat stress: the activation state of Rubisco as a limiting factor in photosynthesis. Physiol Plant 120: 179–186

Salvucci ME, Crafts-Brandner SJ (2004b) Mechanism for deactivation of Rubisco under moderate heat stress. Physiol Plant 122: 513–519

Salvucci ME, Crafts-Brandner SJ (2004c) Inhibition of photosynthesis by heat stress: The activation state of Rubisco as a limiting factor in photosynthesis. Physiol Plant 120: 179–186

Scafaro AP, Bautsoens N, den Boer B, Van Rie J, Gallé A (2019) A Conserved Sequence from Heat-Adapted Species Improves Rubisco Activase Thermostability in Wheat. Plant Physiol 181: 43–54

Scafaro AP, Gallé A, Van Rie J, Carmo-Silva E, Salvucci ME, Atwell BJ (2016) Heat tolerance in a wild Oryza species is attributed to maintenance of Rubisco activation by a thermally stable Rubisco activase ortholog. New Phytol 211: 899–911

Secchi F, Zwieniecki MA (2016) Accumulation of sugars in the xylem apoplast observed under water stress conditions is controlled by xylem pH. Plant Cell Environ 39: 2350–2360

Secchi F, Zwieniecki MA (2011) Sensing embolism in xylem vessels: The role of sucrose as a trigger for refilling. Plant, Cell Environ 34: 514–524

Shivhare D, Mueller-Cajar O (2017) In vitro characterization of thermostable CAM rubisco activase reveals a rubisco interacting surface loop. Plant Physiol 174: 1505–1516

Šiffel P, Braunová Z (1999) Release and aggregation of the light-harvesting complex in intact leaves subjected to strong CO_2 deficit. Photosynth Res 61: 217–226

Šiffel P, Vácha F (1998) Aggregation of the Light-Harvesting Complex in Intact Leaves of Tobacco plants stressed by CO_2 deficit. Photochem Photobiol 67: 304–311

Solís Moya E, Camacho Casas MA (2016) Evaluation of the Stress Adaptive Trait Yield Nursery (SATYN) in irrigated wheat growing locations in Mexico during the 2015-16 growing season. Proc 2nd Int TRIGO Yield Potential 10–14

Stirbet A, Govindjee (2011) On the relation between the Kautsky effect (chlorophyll a fluorescence induction) and Photosystem II: Basics and applications of the OJIP fluorescence transient. J Photochem Photobiol B Biol 104: 236–257

Strasser RJ, Tsimilli-Michael M, Srivastava A (2004) Analysis of the Chlorophyll a Fluorescence Transient. In: Papageorgiou GC, Govindjee (eds) Chlorophyll a Fluorescence. Advances in Photosynthesis and Respiration, vol 19. Springer, Dordrecht

Takahashi S, Murata N (2008) How do environmental stresses accelerate photoinhibition? Trends Plant Sci 13: 178–182

Tang Y, Wen X, Lu Q, Yang Z, Cheng Z, Lu C (2007) Heat stress induces an aggregation of the light-harvesting complex of photosystem II in spinach plants. Plant Physiol 143: 629–38.

Tiwari A, Jajoo A, Bharti S (2008) Heat-induced changes in the EPR signal of tyrosine D (Y(D)OX) a possible role of Cytochrome b559. J Bioenerg Biomembr 40: 237–243

662 Tricker PJ, Elhabti A, Schmidt J, Fleury D (2018) The physiological and genetic basis of combined
663   drought and heat tolerance in wheat. J Exp Bot 69: 3195–3210

664 Trouverie J, Thévenot C, Rocher JP, Sotta B, Prioul JL (2003) The role of abscisic acid in the response
665   of a specific vacuolar invertase to water stress in the adult maize leaf. J Exp Bot 54: 2177–2186

666 Tsimilli-Michael M, Strasser RJ (2008) In vivo assessment of stress impact on plant's vitality:
667   Applications in detecting and evaluating the beneficial role of mycorrhization on host plants. In:
668   Mycorrhiza: State of the Art, Genetics and Molecular Biology, Eco-Function, Biotechnology,
669   Eco-Physiology, Structure and Systematics, 3rd edn. Springer-Verlag Berlin Heidelberg, pp 679–
670   703

671 von Caemmerer S, Farquhar GD (1981) Some relationships between the biochemistry of photosynthesis
672   and the gas exchange of leaves. Planta 153: 376–387

673 Walker BJ, VanLoocke A, Bernacchi CJ, Ort DR (2016) The Costs of Photorespiration to Food
674   Production Now and in the Future. Annu Rev Plant Biol 67: 107–129

675 Wang D, Fu A (2016) The Plastid Terminal Oxidase is a Key Factor Balancing the Redox State of
676   Thylakoid Membrane. In: Enzymes. Academic Press, pp 143–171

677 Wang L, Zheng Y, Ding S, Zhang Q, Chen Y, Zhang J (2017) Molecular cloning, structure, phylogeny
678   and expression analysis of the invertase gene family in sugarcane. BMC Plant Biol 17: 109

679 Weiszmann J, Fürtauer L, Weckwerth W, Nägele T (2018) Vacuolar sucrose cleavage prevents
680   limitation of cytosolic carbohydrate metabolism and stabilizes photosynthesis under abiotic stress.
681   FEBS J 285: 4082–4098

682 Yamamoto Y (2016) Quality Control of Photosystem II: The Mechanisms for Avoidance and Tolerance
683   of Light and Heat Stresses are Closely Linked to Membrane Fluidity of the Thylakoids. Front
684   Plant Sci 7: 1136

685 Zampieri M, Ceglar A, Dentener F, Toreti A (2017) Wheat yield loss attributable to heat waves, drought
686   and water excess at the global, national and subnational scales. Environ Res Lett 12

687 Zandalinas SI, Mittler R, Balfagón D, ArbonaV, Gómez-Cadenas A (2018) Plant adaptations to the
688   combination of drought and high temperatures. Physiol Plant 162: 2–12

689 Zhao C, Liu B, Piao S, et al (2017) Temperature increase reduces global yields of major crops in four
690   independent estimates. Proc Natl Acad Sci USA 114: 9326–9331

691
692
693
694
695
696
697
698

Table 1. Leaf and soil water status, and canopy temperature of Paragon and Sokoll wheat plants exposed to a combination of heat stress and water deficit and recovery from heat stress conditions. Plants were grown for 3 weeks, then exposed to heat stress (38°C versus control, 25°C), water deficit (WD versus well-watered WW) and re-watered at control temperature (25°C) after heat stress conditions (RWW38°C and RWD38°C). Values are means ± SD (n = 5 biological replicates). Different letters denote statistically significant differences between treatments (Duncan analysis, $P<0.05$). LRWC- leaf relative water content; LWP- leaf water potential; SRWC- soil relative water content; Tcanopy- canopy temperature.

| Treatment		Genotype	LRWC (% H_2O)	LWP (MPa)	SRWC (% H_2O)	Tcanopy (°C)
25 °C	WW	Paragon	90.11 ± 8.82 c	-0.50 ± 0.08 c	88.45 ± 5.84 c	26.87 ± 0.65 a
		Sokoll	90.20 ± 1.73 c	-0.81 ± 0.12 bc	80.11 ± 4.88 b	26.33 ± 0.19 a
	WD	Paragon	68.24 ± 12.45 b	-1.16 ± 0.16 ab	26.74 ± 4.84 a	28.79 ± 0.62 b
		Sokoll	31.89 ± 8.87 a	-1.39 ± 0.10 a	29.12 ± 0.92 a	27.89 ± 1.10 b
38 °C	WW	Paragon	78.60 ± 8.47 bc	-0.82 ± 0.06 bc	87.57 ± 2.11 c	35.04 ± 0.98 c
		Sokoll	80.38 ± 4.74 bc	-0.77 ± 0.09 bc	75.02 ± 5.32 b	33.37 ± 0.40 d
	WD	Paragon	39.60 ± 17.71 a	-1.30 ± 0.59 a	30.44 ± 1.69 a	36.95 ± 0.74 e
		Sokoll	43.06 ± 26.64 a	-1.55 ± 0.58 a	28.42 ± 2.72 a	37.52 ± 0.47 e
Recovery	RWW 38 °C	Paragon	86.46 ± 1.36 c	-0.76 ± 0.03 bc	90.13 ± 5.25 c	25.71 ± 0.3 a
		Sokoll	94.91 ± 4.82 cd	-0.74 ± 0.05 bc	91.69 ± 6.14 c	25.58 ± 0.4 a
	RWD 38 °C	Paragon	90.83 ± 3.42 c	-0.72 ± 0.1 bc	88.96 ± 4.1 c	26.33 ± 0.44 a
		Sokoll	78.31 ± 21.18 bc	-0.98 ± 0.16 ab	89.3 ± 3.22 c	26.43 ± 0.21 a
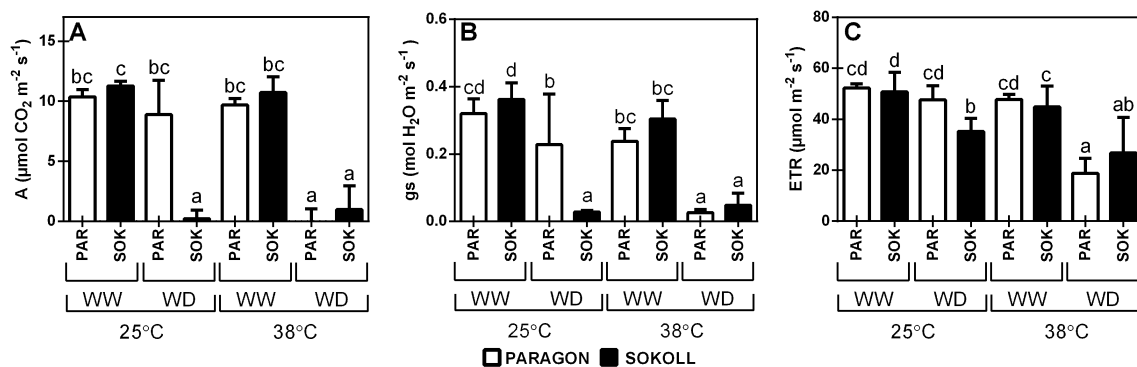
Figure 1. Steady-state photosynthesis of Paragon (PAR) and Sokoll (SOK) wheat plants exposed to a combination of heat stress and water deficit. (A) Net CO_2 assimilation, (B) stomatal conductance (gs) and (C) electron transport rate (ETR) were measured at growth light and ambient CO_2 in fully expanded leaves of wheat 3-week-old plants under well-watered (WW) and water deficit (WD) conditions and exposed to control (25°C) and heat stress conditions (38°C). Values are means ± SD (n = 5 biological replicates). Different letters denote statistically significant differences between treatments (Duncan analysis, $P<0.05$).
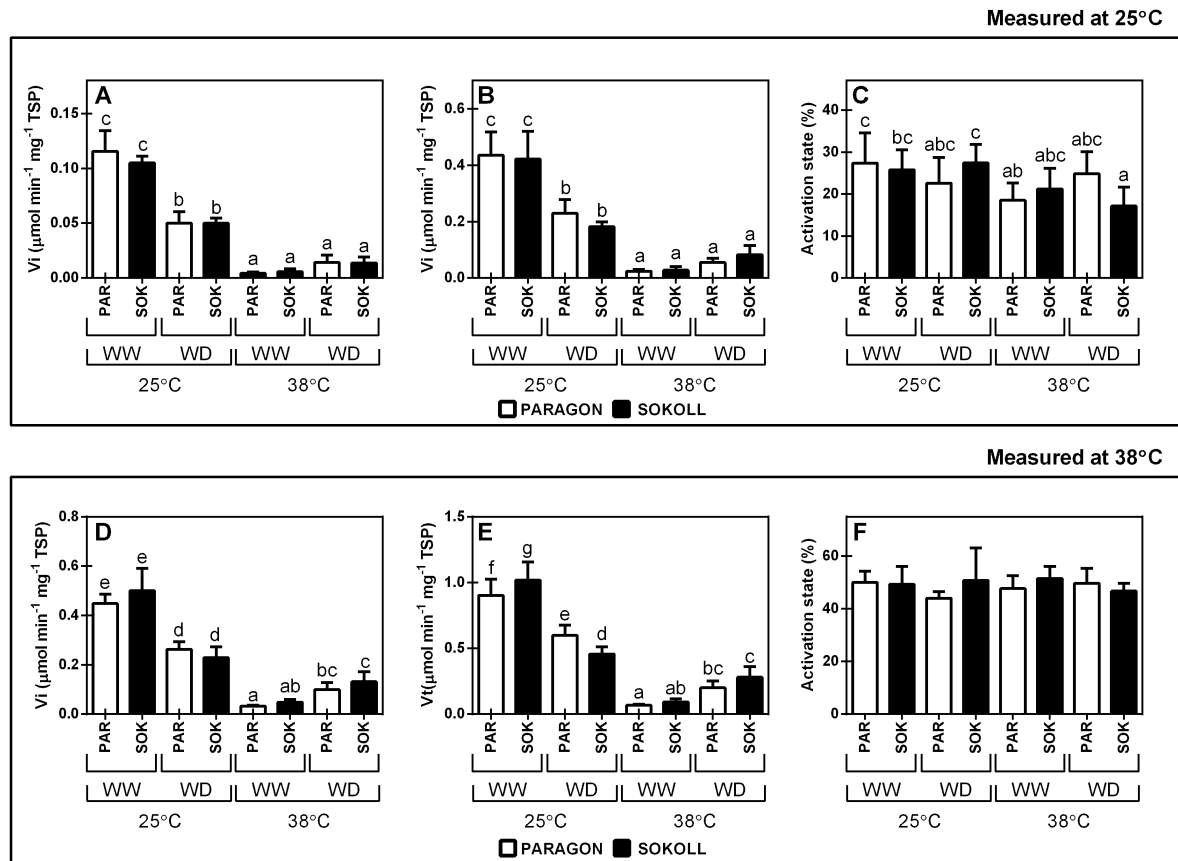
Figure 2. Effect of high temperature and drought on Rubisco activity (expressed by total soluble protein, TSP) and activation state in two wheat genotypes, Paragon (PAR) and Sokoll (SOK). (A-C) Rubisco initial (Vi) and total (Vt) activities and activation state were measured at 25°C and (D-F) 38°C in extracts of fully expanded leaves from 3-week-old wheat plants under well-watered (WW) and water deficit (WD) conditions and exposed to control (25°C) and heat stress conditions (38°C). Values are means ± SD (n = 4-5 biological replicates). Different letters denote statistically significant differences between treatments (Duncan analysis, *P*<0.05).

725
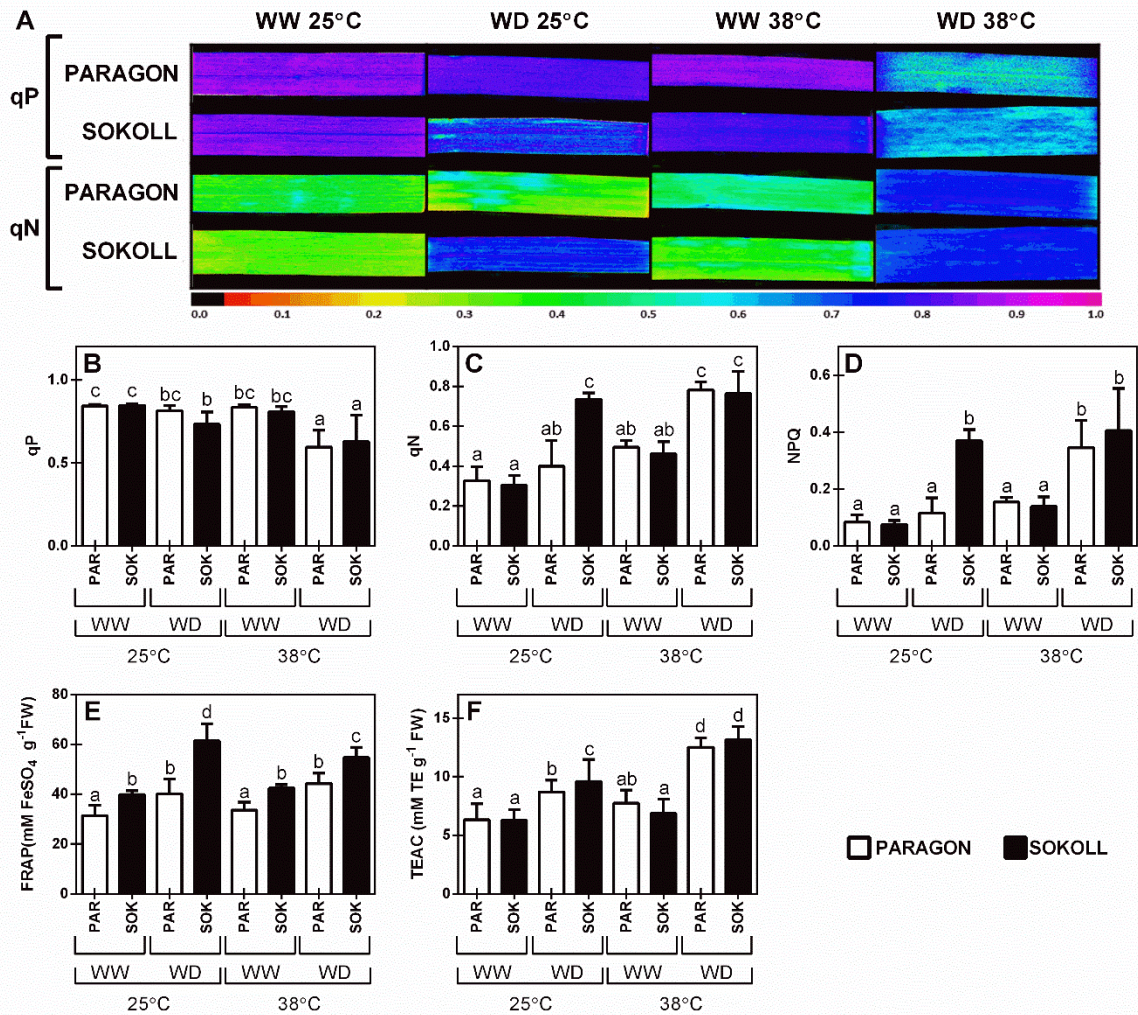
Figure 3. Effect of high temperature and drought on chlorophyll *a* fluorescence and the antioxidant scavenging capacity in two wheat genotypes, Paragon (PAR) and Sokoll (SOK). (A) Chlorophyll *a* fluorescence imaging of the photochemical (qP) and non-photochemical (qN) quenching components in representative leaves. (B) Photochemical quenching (qP), (C) non-photochemical quenching (qN) (D) total non-photochemical quenching (NPQ), (E) ferric reducing antioxidant power (FRAP) and (F) trolox equivalents antioxidant capacity (TEAC) in fully expanded leaves of 3-week-old wheat plants under well-watered (WW) and water deficit (WD) conditions and exposed to control (25°C) and heat stress conditions (38°C). Values are means ± SD (n = 4-5 biological replicates). Different letters denote statistically significant differences between treatments (Duncan analysis, *P*<0.05).
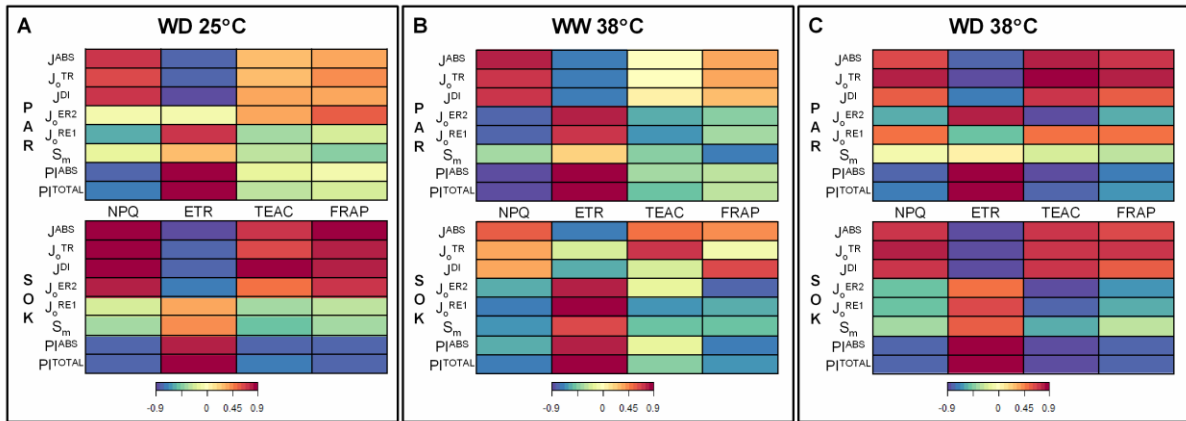
Figure 4. Heatmap representation of the correlation between chlorophyll *a* fluorescence kinetics (OJIP parameters) and antioxidant capacity or steady-state chlorophyll *a* fluorescence of two wheat genotypes, Paragon (PAR) and Sokoll (SOK), under different stresses. Canonical correlations were determined according to the effect of (A) water deficit (at 25°C, WD25°C), (B) high temperatures (well-watered, WW38°C), and (C) water deficit combined with high temperatures (WD38°C) relative to control plants (WW25°C). All parameters were measured in fully expanded leaves of 3-week-old plants. OJIP parameters included are: absorbed photon flux (J^{ABS}); maximum trapped exciton flux (J_o^{TR}); dissipated energy flux (J^{DI}); electron transport flux from Q_A to Q_B (J_o^{ET2}); electron transport flux until PSI acceptors (J_o^{RE1}); number of electron carriers per electron transport chain (S_m); performance index for energy conservation from photons absorbed by PSII antenna to the reduction of QB (PI^{ABS}) and until the reduction of PSI acceptors (PI^{TOTAL}). Mean values ± SD (n = 5 biological replicates) are in supplementary data, Table S1. Steady-state chlorophyll *a* fluorescence parameters are non-photochemical quenching (NPQ) and electron transport rate (ETR). Antioxidant capacity was determined by trolox equivalents antioxidant capacity (TEAC) and ferric reducing antioxidant power (FRAP). Different colours denote positive (red) or negative (blue) correlations between variables (n=5 biological replicates).
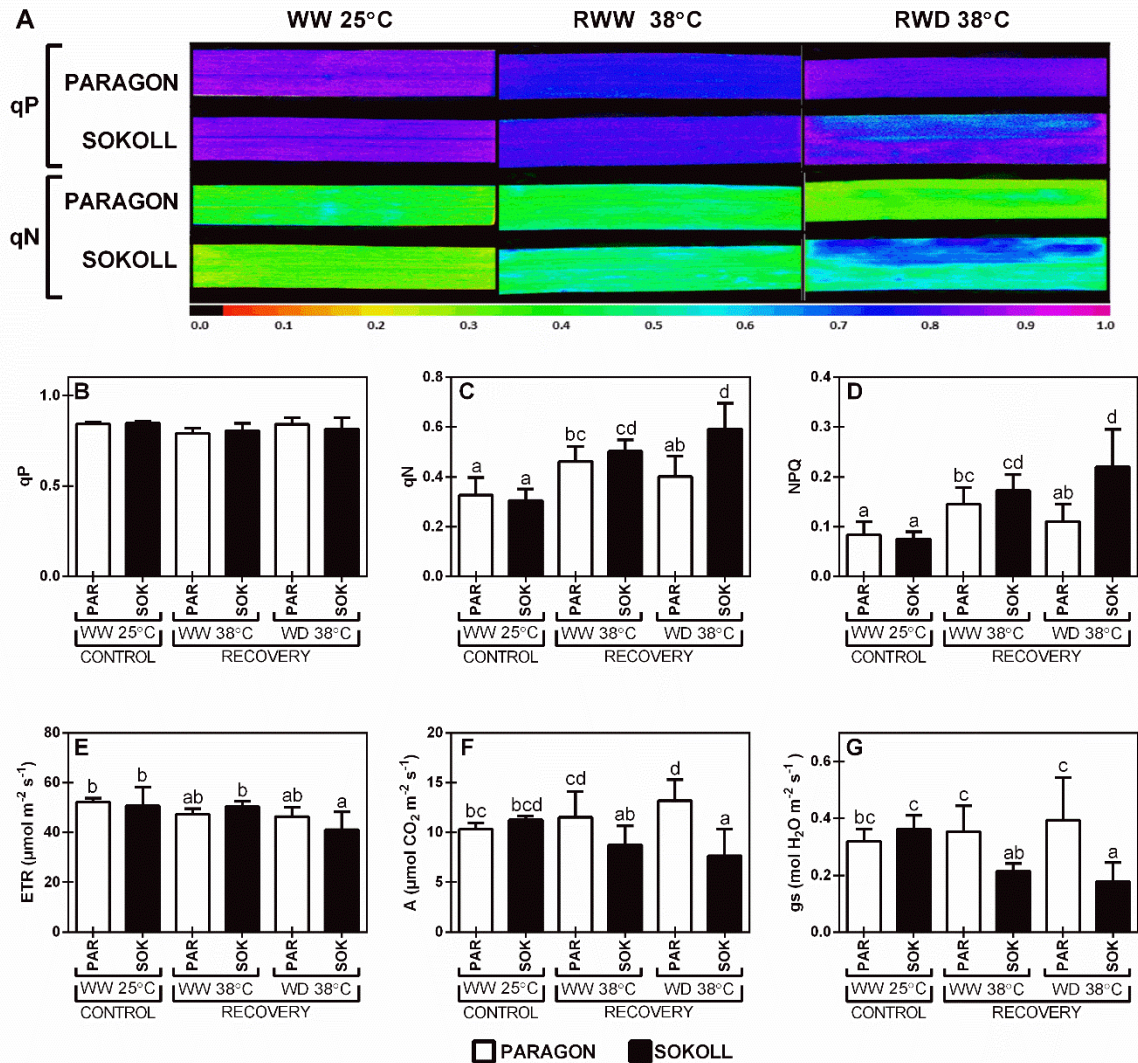
Figure 5. Recovery of the photochemistry and stomatal function of two wheat genotypes, Paragon (PAR) and Sokoll (SOK), after exposure to high temperatures and water deficit. (A) Chlorophyll *a* fluorescence imaging of the photochemical (qP) and non-photochemical (qN) quenching components in representative leaves. (B) Photochemical quenching (qP), (C) non-photochemical quenching (qN), (D) total non-photochemical quenching (NPQ), (E) electron transport rate (ETR), (F) net photosynthetic assimilation rate (A), (G) stomatal conductance (gs). Measurements at growth PPFD in fully expanded leaves of 33-day-old wheat plants recovering for 7 days under well-watered (WW) conditions and 25°C after exposure to WW (RWW 38°C) or water deficit (RWD 38°C) conditions and high temperature (38°C) for 5 days. Values are means ± SD (n=5 biological replicates). Different letters denote statistically significant differences between treatments (Duncan analysis, *P*<0.05).

763
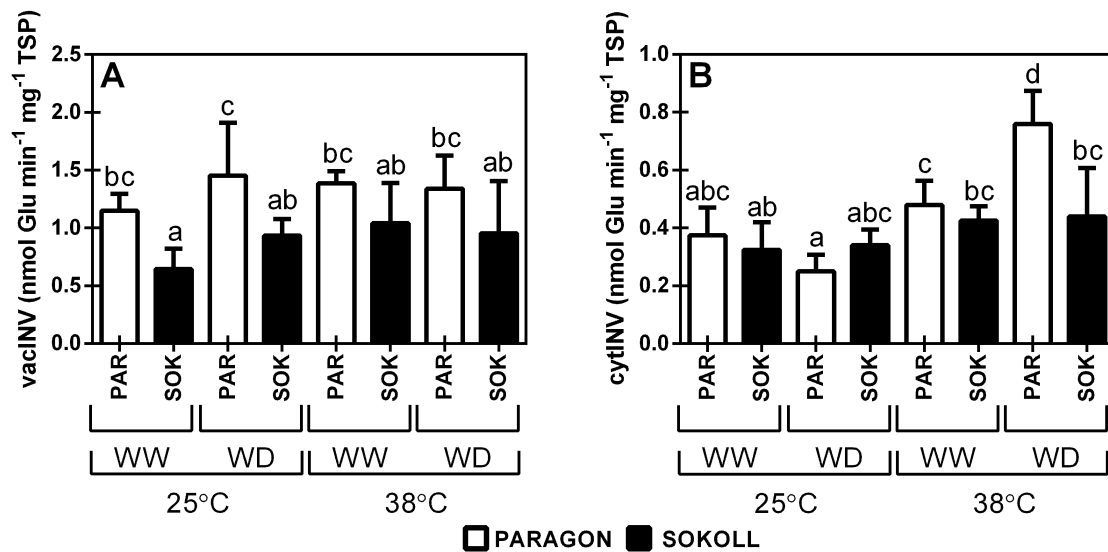
Figure 6. Effect of high temperature and water deficit on cytoplasmic and vacuolar invertases activities in two wheat genotypes, Paragon (PAR) and Sokoll (SOK). (A) Vacuolar Invertase (vacINV) and (B) cytoplasmic invertase (cytINV) activities were measured at 30°C in fully expanded leaves of 3-week-old wheat plants under well-watered (WW) and water deficit (WD) conditions and exposed to control (25°C) and high temperatures (38°C). Values are means ± SD (n=4-5 biological replicates). Different letters denote statistically significant differences between treatments (Duncan analysis, $P<0.05$).

Supplementary data

Fig.S1. Effect of high temperature and drought on Rubisco activity (expressed by leaf area) and activation state in two wheat genotypes, Paragon (PAR) and Sokoll (SOK).

Table S1. Pearson correlation matrix between net photosynthetic assimilation rate (A), stomatal conductance (gs), electron transport rate (ETR) and cytoplasmic invertase (cytINV) in two wheat genotypes, Paragon and Sokoll, under well-watered (WW) and water deficit (WD) conditions and exposed to control (25°C) and high temperatures (38°C).

Table S2. OJIP parameters of Paragon and Sokoll wheat plants exposed to a combination of heat stress and water deficit and recovered under well-watered conditions.

Fig.S2. Chlorophyll *a* fluorescence induction curves (OJIP curves) of Paragon and Sokoll wheat plants exposed to water deficit, heat stress, a combination of heat stress and water deficit and recovered under well-watered conditions.